Published in final edited form as:
Virology. 2012 October 10; 432(1): 120–126. doi:10.1016/j.virol.2012.06.006.

Human Papillomavirus Type 16 E7 oncoprotein engages but does not abrogate the mitotic spindle assembly checkpoint

Yueyang Yu and **Karl Munger**[#]
Division of Infectious Diseases, Brigham and Women's Hospital and Biological and Biomedical Sciences Program, Harvard Medical School, Boston, Massachusetts, 02115

Abstract

The mitotic spindle assembly checkpoint (SAC) ensures faithful chromosome segregation during mitosis by censoring kinetochore-microtubule interactions. It is frequently rendered dysfunctional during carcinogenesis causing chromosome missegregation and genomic instability. There are conflicting reports whether the HPV16 E7 oncoprotein drives chromosomal instability by abolishing the SAC. Here we report that degradation of mitotic cyclins is impaired in cells with HPV16 E7 expression. RNAi-mediated depletion of Mad2 or BubR1 indicated the involvement of the SAC, suggesting that HPV16 E7 expression causes sustained SAC engagement. Mutational analyses revealed that HPV16 E7 sequences that are necessary for retinoblastoma tumor suppressor protein binding as well as sequences previously implicated in binding the Nuclear and Mitotic Apparatus (NuMA) protein and in delocalizing dynein from the mitotic spindle contribute to SAC engagement. Importantly, however, HPV16 E7 does not markedly compromise the SAC response to microtubule poisons.

Keywords

Human Papillomaviruses; E7 oncoprotein; Mitosis; spindle assembly checkpoint; Cervical cancer; Cyclin B

INTRODUCTION

During mitosis, the cell has to equally segregate replicated chromosomes into the two daughter cells. Kinetochores, complex protein assemblies on the centromeres of chromosomes, allow for chromosomes to be captured by microtubules emanating from the two spindle poles, which is necessary for chromosome segregation. Capturing of kinetochores by microtubules is by "trial-and-error" and is monitored by the mitotic spindle assembly checkpoint (SAC). The SAC guards genomic integrity by delaying mitotic chromosome segregation until all chromosomes are properly attached by spindle microtubules. Chromosome segregation and mitotic exit require that the mitotic regulators securin and cyclin B be ubiquitinated by the E3 ubiquitin ligase anaphase promoting complex/cyclosome (APC/C) before being targeted for degradation by the proteasome. The

[#]Corresponding author: Mailing Address: 181 Longwood Ave., MCP 861, Boston, MA 02215. Phone (617) 525-4282, Fax (617) 525-4283, kmunger@rics.bwh.harvard.edu.

SAC thus comes into play in prometaphase by sequestering the APC/C coactivator CDC20 and preventing it from activating APC/C (reviewed in (Musacchio and Salmon, 2007)).

Studies with anti-microtubule drugs in yeast identified genes necessary for the SAC as early as two decades ago. These genes were named *mitotic arrest deficient (MAD)* and *budding uninhibited by benzimidazole (BUB)* (Hoyt et al., 1991; Li and Murray, 1991). Evolutionarily conserved from yeast to human, the key cytosolic SAC effectors Mad2 (MAD2L1), BubR1 (BUB1B) and BUB3 form a complex with CDC20, known as the mitotic checkpoint complex (MCC). Depletion of checkpoint proteins including Mad2, BubR1, and BUB3 have been shown to abolish the SAC (Meraldi et al., 2004). SAC dysfunction has been linked to development of aneuploidy during tumorigenesis by studies with human cancer cell lines with SAC gene mutations and mouse models of SAC deficiency. Moreover, several tumor suppressors and oncogenes regulate expression and/or activity of SAC proteins (reviewed in (Suijkerbuijk and Kops, 2008)).

Human papillomaviruses (HPVs) are small DNA viruses that infect squamous epithelia of the skin or mucous membranes. HPVs infect the proliferating basal cell layer through microabrasions or at squamocolumnar transformation zones where basal-like cells are exposed. HPV genomes are maintained as episomes and the productive phase of the viral life cycle occurs exclusively in differentiated cells. Since HPVs are acutely dependent on cellular replication factors, HPVs need to uncouple the proliferation/differentiation switch, an activity that is mainly executed by the E7 protein. Malignant progression of high-risk HPV-associated lesions is a relatively rare event, and is accompanied by accumulation of structural and numerical chromosome aberrations. The high-risk HPV E6 and E7 proteins, which are consistently expressed in HPV-associated lesions and cancers, have been shown to induce genomic instability through a number of different mechanisms (reviewed in (Klingelhutz and Roman, 2012; McLaughlin-Drubin and Munger, 2009)).

HPV16 E7 not only overcomes G1/S checkpoint restriction by targeting the retinoblastoma tumor suppressor (pRB) for proteasomal degradation (Huh et al., 2007), but also drives genomic destabilization. HPV16 E7 expression causes synthesis of supernumerary centrosomes, chromosome alignment delays, and persistent presence of double strand DNA breaks (Duensing et al., 2001; Duensing and Munger, 2002; Nguyen and Munger, 2009), each of which is likely to impair the fidelity of mitosis and trigger SAC activation. Several studies have suggested that HPV16 E7 expression abrogates the SAC, with cells escaping prolonged mitotic arrest and developing polyploidy in the presence of microtubule poisons (Patel et al., 2004; Thomas and Laimins, 1998). There is also the opposite view that instead of abrogating the SAC, HPV16 E7 abolishes a postmitotic checkpoint, which becomes active and prevents further cell cycle progression when cells adapt to the SAC, decondense their chromosomes and undergo mitotic slippage to a G1-like state with 4N DNA (Heilman et al., 2009; Khan and Wahl, 1998).

Previous live-cell imaging studies in our lab revealed a prometaphase delay in cells with HPV16 E7 expression (Nguyen and Munger, 2009), suggestive of SAC activation. Here we report that the expression of HPV16 E7 impedes the degradation of mitotic cyclins and that this is in part dependent on E7 mediated SAC engagement. We also demonstrate the functionality of the SAC in response to microtubule poisons in cells with HPV16 E7 expression. We hypothesize that a functional SAC may contribute to the viral life cycle by ensuring viral genome persistence.

RESULTS

HPV16 E7 expression impedes cyclin B degradation during mitosis

Previous immunofluorescence and live-cell imaging studies in our lab demonstrated a prometaphase delay associated with HPV16 E7 expression (Nguyen and Munger, 2009). Despite earlier reports that linked the expression of HPV16 E7 alone or together with HPV16 E6 to the abrogation of the SAC (Patel et al., 2004; Thomas and Laimins, 1998), we did not observe frequent conversion of delayed chromosome congression in E7-expressing cells during metaphase into lagging chromosomes in anaphase (Nguyen and Munger, 2009). This led us to hypothesize that the SAC is still functional in HPV16 E7-expressing cells. To address this, we examined the degradation of cyclin B in mitosis, which is directly inhibited by the SAC (Musacchio and Salmon, 2007), in HPV16 E7-expressing cells.

Colon carcinoma RKO cells were initially used for these experiments because they have wild type p53 and pRB tumor suppressor activity and an intact SAC (Cahill et al., 1998). Moreover, clonal RKO lines with high-level HPV16 E7 expression have been described (Slebos et al., 1994) (Fig 1A). To compare cell cycle progression of HPV16 E7-expressing RKO cells (RKO E7) to control vector transfected cells (RKO C), cells were subjected to a double thymidine block, which causes a G1/S arrest. We performed cell cycle analyses by FACS after propidium iodide staining and quantified the percentage of G2/M cells (4N DNA). RKO C and RKO E7 cells responded equally well to double thymidine synchronization, with only ~10% of cells in G2/M at the time of release from double thymidine block (Fig 1B). After release from the double thymidine block we investigated the mitotic markers phospho histone H3 serine 10 (pH3S10) and cyclin B for a time period of 14 hours, during which most RKO C and RKO E7 cells synchronously progressed through G2 and M phase (Fig 1B). Cyclin B levels peaked at 8 hours and 10 hours post release in RKO C and RKO E7 cells, respectively, consistent with the high levels of pH3S10 at these time points. By 14 hours post release, cyclin B levels decreased by 56% from its peak levels in RKO C cells, while only an 18% decrease was observed in RKO E7 cells, suggesting that cyclin B degradation during mitosis may be inhibited in RKO E7 cells (Fig 1A).

We decided to use primary human foreskin fibroblasts (HFFs) for more detailed analyses of SAC engagement in response to HPV16 E7 expression. HFFs were used for several reasons: Even though RKO cells retain SAC function (Cahill et al., 1998) they are a cancer derived line and may contain mutations that affect the proper functioning of the SAC. In addition, the fact that RKO C and RKO E7 cells exhibited slightly different timing of G2/M or mitotic peaks by FACS (Fig 1B) and cyclin B peaks by Western blots (Fig 1A) complicates our interpretation that cyclin B degradation is inhibited during mitosis and may simply reflect delayed accumulation of cyclin B prior to the metaphase-to-anaphase transition in RKO E7 cells. Whereas keratinocytes, not fibroblasts are the natural host cells of HPVs, HFFs have a higher mitotic index than keratinocytes, which makes them amenable to mitotic analyses as well as double thymidine synchronization.

We generated donor and passage matched primary HFF populations infected with empty vector (HFF C) or HPV16 E7 (HFF E7) (Fig 2A). The two cell populations were arrested at the G1/S boundary by double thymidine block and, after release, we followed their passage through the cell cycle by FACS (Fig 2B). In HFF C, cyclin B levels peaked at 8 hours after release from double thymidine block and decreased by 76% by 14 hours post release. In HFF E7, cyclin B levels also peaked at 8 hours post release but decreased by only 59% by 14 hours post release (Fig 2C). Moreover, cyclin B levels were already markedly higher in double thymidine block G1/S arrested HFF E7 cells than in HFF C cells (~2 fold difference,

Fig 2C). Hence these experiments demonstrate that HPV16 E7 expression impedes the mitotic degradation of cyclin B in primary HFFs.

The pRB-binding domain as well as C-terminal HPV16 E7 sequences are necessary for the impairment of mitotic cyclin B degradation

To determine which functions of HPV16 E7 may contribute to inhibition of cyclin B degradation, we assessed HFFs expressing wild-type E7, or the HPV16 E7Δ21-24 and HPV16 E7Δ79-83 mutants. The pRB family binding deficient HPV16 E7Δ21-24 and the $p21^{CIP1}$ and $p27^{KIP1}$ binding defective HPV16 E7Δ79-83 mutants (Funk et al., 1997; Zerfass-Thome et al., 1996) have been previously characterized for their abilities to induce disorganized metaphases, which presumably represents a prometaphase delay (Nguyen and Munger, 2009).

Even though the two E7 mutants did not appear to be expressed at the same levels as wild-type E7 by Western blot (Fig 3A), pRB levels were similarly decreased in wild type HPV16 E7 and HPV16 E7Δ79-83 mutant expressing HFFs (Fig 3B) suggesting that the HPV16 E7Δ79-83 mutant was expressed at levels that were sufficient for functionality. The HPV16 E7Δ21-24 mutant is not recognized by the ED17 antibody (Psyrri et al., 2004), which may result in decreased detection of this mutant in our Western blots. HFFs with stable expression of empty vector, wild-type E7, E7Δ21-24, and E7Δ79-83 exhibited similar cell cycle profiles after release from a double thymidine block (Fig 3C). Consistent with what we observed before (Fig 2), HPV16 E7 expression impeded mitotic cyclin B degradation, with cyclin B levels decreasing by 47% from 8 hours to 14 hours post release, compared to an 89% decrease over the same period of time in HFF C. Similar to HFF C, cyclin B levels decreased by 80% and 90% in HFFs expressing the HPV16 E7Δ21-24 and HPV16 E7Δ79-83 mutants, respectively. Therefore, both the pRB-binding domain and C-terminal HPV16 E7 sequences contribute to inhibition of mitotic cyclin B degradation.

HPV16 E7 engages SAC-dependent and -independent pathways to impede the degradation of mitotic cyclins

In order to address whether engagement of the SAC accounts for E7 mediated inhibition of cyclin B degradation during mitosis, we transfected HFF C and HFF E7 with siRNA pools targeting the SAC effectors Mad2 or BubR1 before synchronizing the cells for cell cycle analyses. Both Mad2 and BubR1 expression was efficiently reduced after siRNA transfection (Fig 4). Cyclin B was more efficiently degraded in HFF E7 cells after depletion of Mad2 (45%) or BubR1 (48%) as compared to control siRNA transfected cells (31%) (Fig 4). We also assessed steady state levels of cyclin A, an APC/C substrate not subject to SAC regulation (den Elzen and Pines, 2001; Geley et al., 2001). In HFF C, cyclin A levels decreased by 70% at 14 hours post release from a double thymidine block, whereas the decrease was only 29% in HFF E7 cells. Cyclin A levels did not decrease more efficiently in HFF E7 cells upon depletion of Mad2 (0%) or BubR1 (18%) (Fig 4). Hence, we conclude that HPV16 E7 engages both SAC-dependent and SAC-independent mechanisms to impede the degradation of mitotic cyclins.

HPV16 E7 expression does not compromise the SAC response to microtubule poisons

Our experiments so far revealed that in a synchronized but otherwise unperturbed cell cycle, cyclin B degradation did not proceed as efficiently in HPV16 E7-expressing cells as in control cells, and this was in part dependent on a functional SAC. We therefore decided to also examine the SAC response to microtubule poisons, a standard laboratory test for SAC activity. We arrested HFF C and HFF E7 cells at the G1/S boundary by a single thymidine block before treatment with nocodazole or taxol for 18 hours (Fig 5A). This time was chosen because cells do not remain arrested in M phase for extended periods of time but

eventually undergo mitotic slippage to a tetraploid G1-like state (Taylor and McKeon, 1997). The nocodazole concentrations that we tested included the 50 ng/ml dose that was used in a previous report suggesting that HPV16 E7 expression bypassed the SAC (Thomas and Laimins, 1998) as well as a higher dose of 200 ng/ml that was used to document mitotic arrest followed by slippage from mitosis after 18 hours (Taylor and McKeon, 1997). We also tested a range of taxol concentrations that have been shown in previous studies to allow for differential detection of various degrees of SAC defects (Wang et al., 2010).

Only 1.1% of HFF C and 1.5% of HFF E7 were in mitosis in DMSO treated cells at 18 hours post release from the thymidine block (p=0.48). HFF C and HFF E7 cells arrested in mitosis with similar efficiencies at all nocodazole concentrations tested, with HFF E7 performing slightly better although these differences were not significant statistically (at 50 ng/ml: 41.8% HFF E7 compared to 34.4% HFF C, p=0.13; at 100 ng/ml: 41.3% HFF E7 compared to 34.3% HFF C, p=0.1; at 200 ng/ml: 38.3% HFF E7 compared to 32.6% HFF C, p=0.19). The range of taxol concentrations tested rendered a dose response of arrest efficiency, and at all concentrations HFF E7 showed somewhat higher degrees of mitotic arrest, although these were not statistically significant (at 33 nM: 14.8% HFF E7 compared to 13.9% HFF C, p=0.54; at 100 nM: 23.4% HFF E7 compared to 16.2% HFF C, p=0.14; at 1000 nM: 50.4% HFF E7 compared to 45.6% HFF C, p=0.39).

Previous experiments reporting subversion of the SAC by HPV16 E7 expression were performed with primary human foreskin keratinocytes (HFKs) (Patel et al., 2004; Thomas and Laimins, 1998). Therefore, we generated donor and passage matched primary HFK populations infected with empty vector (HFK C) or HPV16 E7 (HFK E7). Since we could not achieve good thymidine synchronization with HFKs, we treated the cells with various concentrations of nocodazole and taxol for 24 hours without prior thymidine treatment (Fig 5B). As expected, DMSO-treated HFKs had lower mitotic indices than HFFs. HFK C and HFK E7 cells arrested with similar efficiencies in nocodazole (at 50 ng/ml: 4.3% HFK E7 compared to 4.5% HFK C, p=0.9; at 100 ng/ml, 5.9% HFK E7 compared to 5.6% HFK C, p=0.57; at 200 ng/ml, 7.2% HFK E7 compared to 6.2% HFK C, p=0.23). Interestingly, however, HFK E7 showed statistically higher degrees of mitotic arrest in taxol (at 33 nM, 12.1% HFK E7 compared to 9.9% HFK C, p=0.03; at 100 nM, 12.2% HFK E7 compared to 9.2% HFK C, p=0.005; at 1000 nM, 9.1% HFK E7 compared to 6.8% HFK C, p=0.02).

In conclusion, equally robust or sometimes higher degrees of mitotic arrest in response to microtubule poisons suggested that HPV16 E7 expression in primary human fibroblasts or keratinocytes does not impair the SAC or drive mitotic slippage in primary cells in response to nocodazole or taxol treatment.

DISCUSSION

Previous studies in our lab hinted at the possibility that the SAC may remain functional in HPV16 E7-expressing cells. Despite the increased incidence of disorganized metaphases in HPV16 E7-expressing cells under fixed conditions revealed by immunofluorescence, live-cell imaging experiments suggested that these disorganized metaphases actually represented a prometaphase delay and that such cells eventually progressed into normal meta- and anaphases (Nguyen and Munger, 2009). Here we show that mitotic cyclin B degradation is impaired by HPV16 E7 expression in a synchronized but otherwise unperturbed cell cycle (Fig 1&2). This result suggests that HPV16 E7 expression may trigger the SAC, which directly inhibits cyclin B degradation. One caveat of this interpretation is that E7 encoded by another high-risk HPV, HPV18, has been reported to cause a prolonged G2 phase following S phase reentry in raft cultures of differentiated human keratinocytes (Banerjee et al., 2011). Hence, we needed to determine whether the observed sustained cyclin B levels during

mitosis in HPV16 E7 expressing cells may reflect a delay in mitotic entry due to a prolonged G2 phase. Indeed, RKO E7 cells achieved peak cyclin B levels later than RKO C cells (Fig 1). This prompted us to examine primary human fibroblasts with E7 expression. HFF E7 cells progressed through the cell cycle with similar kinetics as HFF C cells after synchronization with a double thymidine block and cyclin B was still not degraded as efficiently in HFF E7 as in HFF C (Fig 2). We observed higher levels of cyclin B in cells with HPV16 E7 expression in late S and G2 (0 and 4 hours after release from a double thymidine block, respectively - Fig 1&2). This is consistent with the model that high-risk HPV E7 upregulates cyclin B expression (Banerjee et al., 2011) and/or causes incomplete degradation of mitotic cyclin B. However, this does not mask the effects of HPV16 E7 on mitotic cyclin B degradation because cyclin B levels accumulated to similar peaks during mitosis in control- and E7-expressing cells (Fig 1&2).

In contrast to wild type HPV16 E7, expression of the pRB family binding/degradation deficient HPV16 E7Δ21-24 and the C-terminal HPV16 E7Δ79-83 mutants did not impede cyclin B degradation (Fig 3). It has been shown that pRB inactivation results in a hyperactive SAC and delayed mitotic progression, and that the deregulated expression of Mad2, an E2F target gene, is an important mediator of this effect (Hernando et al., 2004). Indeed we observed slightly higher Mad2 levels in cells with HPV16 E7 expression (Fig 4). Hence, the reduced inhibition of cyclin B degradation by the HPV16 E7Δ21-24 mutant may reflect that this mutant cannot interact with and degrade pRB and thus will not deregulate Mad2 transcription through E2F. The HPV16 E7Δ79-83 mutant, while competent for pRB degradation (Helt et al., 2002), is defective for dynein delocalization from mitotic spindles and cannot interact with NuMA (Nguyen et al., 2008; Nguyen and Munger, 2009). Dynein is a minus-end directed microtubule motor protein that has been implicated in the inactivation of the SAC by “stripping” checkpoint proteins off the kinetochores via transport along microtubules (reviewed in (Musacchio and Salmon, 2007)). NuMA is involved in mitotic spindle organization and chromosome alignment (Levesque et al., 2003). Accordingly, HPV16 E7 may thwart cyclin B degradation by causing sustained SAC activation through E2F mediated, dysregulated Mad2 expression and by inhibiting dynein-mediated SAC inactivation as well as NuMA function.

We investigated whether E7 triggered SAC engagement contributes to impaired cyclin B degradation by depleting Mad2 or BubR1 in HFF E7 cells (Fig 4). While cyclin B degradation kinetics in Mad2 or BubR1 depleted HFF E7 cells were not completely restored to levels seen in HFF C, it is possible that the residual levels of these checkpoint proteins on the kinetochores, although not readily detectable by Western blotting of whole cell lysates, may still support some SAC signaling. The inability of Mad2 or BubR1 depletion to reverse impaired cyclin A downregulation in HFF E7 cells, however, underlines the specificity of our assay and also points to a SAC-independent aspect of the inhibition of mitotic cyclin degradation by E7. Future studies will examine the degradation of other APC/C substrates such as Aurora B and CDC20 (Peters, 2006) in HPV16 E7-expressing cells. Since E7 has no intrinsic enzymatic activities and perturbs cellular pathways mainly through protein-protein interactions, proteomics studies of E7 in mitotic extracts may provide some clues to the underlying mechanism of how E7 impairs the proteasomal degradation of mitotic cyclins.

We offered direct evidence that the SAC is not impaired by HPV16 E7 expression in response to the microtubule poisons, nocodazole and taxol (Fig 5). The previous studies reporting that HPV16 E7 expression bypassed the SAC triggered by nocodazole may arise from SAC adaptation and mitotic slippage during prolonged drug treatment (Taylor and McKeon, 1997; Thomas and Laimins, 1998). Evidences abound for viral oncoproteins targeting the SAC, including the SV40 large T antigen (Cotsiki et al., 2004), HTLV-1 oncoprotein Tax (Jin et al., 1998), and HBV X protein (Kim et al., 2008). Although

abrogating the SAC can contribute to chromosomal instability by viral oncoproteins, HPV16 E7 expressing cells may need to retain a functional SAC. HPV16 E7 disrupts the organization of a bipolar mitotic spindle through induction of supernumerary centrosomes and by disrupting NuMA function (Duensing et al., 2001; Nguyen and Munger, 2009). HPV16 E7 may also obstruct the chromosome alignment process by associating with NuMA and harboring DNA double strand breaks (Duensing and Munger, 2002; Nguyen and Munger, 2009). A functional or even a sustained SAC due to interference with SAC inactivation by disrupting dynein function (Nguyen et al., 2008) in E7 expressing cells may provide an extended window of time to resolve these potentially lethal genetic abnormalities and achieve faithful chromosome segregation. The ability to undergo mitosis that yields viable daughter cells is essential for HPV infected cells to efficiently maintain and segregate viral episomes.

In conclusion, we have shown that cells with HPV16 E7 expression retain a functional SAC both in a synchronized setting and in response to microtubule poisons. Mitotic errors due to SAC inactivation can result in the generation of nonviable progeny, which would also result in the loss of viral genomes and interfere with persistent infection as well as the viral life cycle. Hence, we hypothesize that sustained SAC activity due to HPV E6 and E7 induced genomic instability may facilitate viable mitosis that is essential for viral genome maintenance.

MATERIALS AND METHODS

Cells

RKO pC (pCMV control cells) and RKO7.6 (E7-expressing) cells (Slebos et al., 1994), a generous gift from Kathleen Cho (University of Michigan, Ann Arbor MI), were maintained in modified McCoy's medium (Gibco Invitrogen) supplemented with 10% newborn calf serum (NCS), 50 U/ml penicillin, 50 μg/ml streptomycin, and 500 μg/ml G418. Primary human foreskin fibroblasts (HFFs) and human foreskin keratinocytes (HFKs) were isolated from anonymous newborn circumcisions as previously described (McLaughlin-Drubin et al., 2008). HFFs with stable expression of wild-type or mutant HPV16 E7 were generated by infecting primary HFF populations with the following pBABE-puromycin-based retroviral vectors: pBABE, pBABE-16E7, pBABE-16E7 Δ21-24 and pBABE-16E7 Δ79-83. Recombinant retroviruses were produced in 293T cells as previously described (Piboonniyom et al., 2003). Infections of 50% confluent HFFs were performed with a mixture of 2 ml viral supernatant, 8 μg/ml Polybrene, and 2 ml Dulbecco's modified Eagle medium (DMEM) for 4–6 hours. The cells were maintained in DMEM supplemented with 10% NCS, 50 U/ml penicillin and 50 μg/ml streptomycin. HFKs with stable expression of HPV16 E7 were generated by retroviral infection with pLXSN based vectors and maintained in keratinocytes serum-free medium (KSFM) supplemented with human recombinant epidermal growth factor 1–53, bovine pituitary extract (Invitrogen), 50 U/ml penicillin and 50 μg/ml streptomycin, 20 μg/ml gentamicin, and 1 μg/ml amphotericin B. All experiments were performed with HFF or HFK populations passaged less than ten times.

Western Blotting and Antibodies

Cells were lysed in ML buffer (300 mM NaCl, 0.5% Nonidet P-40 [NP-40], 20 mM Tris-HCl [pH 8.0], 1 mM EDTA) supplemented with one complete EDTA-free protease inhibitor cocktail tablet (Roche) per 25 ml lysis buffer and one PhosSTOP phosphatase inhibitor cocktail tablet (Roche) per 10 ml lysis buffer. Lysates were cleared by centrifugation at 16,000 × g for 15 min at 4°C. Protein concentrations were determined by Bradford assay (Bio-Rad). Proteins were separated by SDS-PAGE and electro transferred onto polyvinylidene difluoride membranes (Immobilon-P; Millipore). Membranes were blocked

in 5% nonfat dry milk in TNET buffer (200 mM Tris-HCl, 1 M NaCl, 50 mM EDTA, 0.1% Tween 20 [pH 7.5]) or 5% BSA in TBST (137 mM NaCl, 2.7 mM KCl, 25 mM Tris [pH 7.4], 0.1% Tween 20) and probed with appropriate antibodies. The following primary antibodies were used at the indicated dilutions: HPV16 E7 (8C9, Zymed/Invitrogen, 1:150 mixed with ED17, Santa Cruz Biotechnology, 1:200); pRB (AB-5, CalBiochem, 1:100); pH3S10 (ab5176, Abcam, 1:500), histone H3 (9715, Cell Signaling, 1:1,000), cyclin B (610219, BD Transduction Laboratories, 1:1,000), cyclin A (sc-751, Santa Cruz Biotechnology, 1:500), Mad2 (610679, BD Transduction Laboratories, 1:1,000), BubR1 (05–898, Upstate/Millipore, 1:1,000), and actin (MAB1501, Millipore, 1:1,000). Secondary anti-mouse and anti-rabbit antibodies conjugated to horseradish peroxidase were used at a 1:10,000 dilution. Proteins were visualized by enhanced chemiluminescence (Perkin Elmer, Millipore) and exposed on Kodak BioMax XAR film, or electronically acquired with a Kodak Image Station 4000R equipped with Kodak Imaging Software, version 4.0, or with Carestream Gel Logic 4000.

Cell Synchronization and RNAi

RKO and HFF cells were synchronized by a double thymidine block by treating cells with 2 mM thymidine for 18 hours, followed by an 8 hour release in normal medium and treatment with 2 mM thymidine for an additional 16 hours. For siRNA transfection, 1.5×10^5 HFF cells were seeded in 6 cm plates one day before transfection with 200 pmol MAD2L1-specific ON-TARGETplus SMARTpool (L-003271-00-0005; Thermo Scientific Dharmacon) or BUB1B-specific ON-TARGETplus SMARTpool (L-004101-00-0005; Thermo Scientific Dharmacon), or ON-TARGETplus Non-Targeting Pool (D-001810-10-05; Thermo Scientific Dharmacon) using Lipofectamine 2000 (Invitrogen). At one day after siRNA transfection, HFFs were subjected to a double thymidine block and harvested for Western blot analyses.

Flow cytometry

For cell cycle analyses by propidium iodide staining, cells were harvested at different times after release from a double thymidine block and fixed with 70% ice-cold ethanol. Cells were then incubated in 30 μg/ml propidium iodide, 100 μg/ml RNAse A, in phosphate buffered saline (PBS) for 30 min at room temperature in the dark. To specifically quantify mitotic cells in response to drug-induced mitotic arrest, HFFs were treated with 2 mM thymidine for 24 hours followed by nocodazole (Sigma) or taxol (Sigma) treatment at the indicated concentrations for 18 hours. HFKs were treated with nocodazole or taxol at the indicated concentrations for 24 hours. Cells were then fixed with 70% ice-cold ethanol, rinsed with 1% fetal calf serum (FCS) in PBS, stained for MPM-2 (05–368, Upstate/Millipore, 1:1,000) for one hour at room temperature, and with Alexa Fluor® 488 Goat Anti-Mouse IgG (H+L) (Molecular Probes/Invitrogen, 1:400) for one hour at room temperature in the dark followed by propidium iodide staining as described above. Flow cytometry was conducted on a FACSCalibur (Becton Dickinson, Franklin Lakes, NJ). Data were acquired using the CellQuest software (Becton Dickinson) and analyzed with CellQuest or FlowJo 7.6.1.

Acknowledgments

We thank James DeCaprio, Jonathan Higgins, Jagesh Shah, and Ulrike Eggert for helpful discussions, Mark Fogg for technical advice regarding FACS, Margaret McLaughlin-Drubin for sharing wild-type and mutant HPV16 E7-expressing HFFs, Jennifer M. Spangle for sharing HPV16 E7-expressing HFKs, Kathleen Cho for sharing RKO7.6 cells and the Munger laboratory for helpful discussions and support. This work was supported by PHS grants R01 CA066980 and R01 CA081135 (K.M.)

References

Banerjee NS, Wang HK, Broker TR, Chow LT. Human papillomavirus (HPV) E7 induces prolonged G2 following S phase reentry in differentiated human keratinocytes. J Biol Chem. 2011; 286:15473–15482. [PubMed: 21321122]

Cahill DP, Lengauer C, Yu J, Riggins GJ, Willson JK, Markowitz SD, Kinzler KW, Vogelstein B. Mutations of mitotic checkpoint genes in human cancers. Nature. 1998; 392:300–303. [PubMed: 9521327]

Cotsiki M, Lock RL, Cheng Y, Williams GL, Zhao J, Perera D, Freire R, Entwistle A, Golemis EA, Roberts TM, Jat PS, Gjoerup OV. Simian virus 40 large T antigen targets the spindle assembly checkpoint protein Bub1. Proc Natl Acad Sci U S A. 2004; 101:947–952. [PubMed: 14732683]

den Elzen N, Pines J. Cyclin A is destroyed in prometaphase and can delay chromosome alignment and anaphase. J Cell Biol. 2001; 153:121–136. [PubMed: 11285279]

Duensing S, Duensing A, Crum CP, Munger K. Human papillomavirus type 16 E7 oncoprotein-induced abnormal centrosome synthesis is an early event in the evolving malignant phenotype. Cancer Res. 2001; 61:2356–2360. [PubMed: 11289095]

Duensing S, Munger K. The human papillomavirus type 16 E6 and E7 oncoproteins independently induce numerical and structural chromosome instability. Cancer Res. 2002; 62:7075–7082. [PubMed: 12460929]

Funk JO, Waga S, Harry JB, Espling E, Stillman B, Galloway DA. Inhibition of CDK activity and PCNA-dependent DNA replication by p21 is blocked by interaction with the HPV-16 E7 oncoprotein. Genes Dev. 1997; 11:2090–2100. [PubMed: 9284048]

Geley S, Kramer E, Gieffers C, Gannon J, Peters JM, Hunt T. Anaphase-promoting complex/cyclosome-dependent proteolysis of human cyclin A starts at the beginning of mitosis and is not subject to the spindle assembly checkpoint. J Cell Biol. 2001; 153:137–148. [PubMed: 11285280]

Heilman SA, Nordberg JJ, Liu Y, Sluder G, Chen JJ. Abrogation of the postmitotic checkpoint contributes to polyploidization in human papillomavirus E7-expressing cells. J Virol. 2009; 83:2756–2764. [PubMed: 19129456]

Helt AM, Funk JO, Galloway DA. Inactivation of both the retinoblastoma tumor suppressor and p21 by the human papillomavirus type 16 E7 oncoprotein is necessary to inhibit cell cycle arrest in human epithelial cells. J Virol. 2002; 76:10559–10568. [PubMed: 12239337]

Hernando E, Nahle Z, Juan G, Diaz-Rodriguez E, Alaminos M, Hemann M, Michel L, Mittal V, Gerald W, Benezra R, Lowe SW, Cordon-Cardo C. Rb inactivation promotes genomic instability by uncoupling cell cycle progression from mitotic control. Nature. 2004; 430:797–802. [PubMed: 15306814]

Hoyt MA, Totis L, Roberts BT. S. cerevisiae genes required for cell cycle arrest in response to loss of microtubule function. Cell. 1991; 66:507–517. [PubMed: 1651171]

Huh K, Zhou X, Hayakawa H, Cho JY, Libermann TA, Jin J, Harper JW, Munger K. Human papillomavirus type 16 E7 oncoprotein associates with the cullin 2 ubiquitin ligase complex, which contributes to degradation of the retinoblastoma tumor suppressor. J Virol. 2007; 81:9737–9747. [PubMed: 17609271]

Jin DY, Spencer F, Jeang KT. Human T cell leukemia virus type 1 oncoprotein Tax targets the human mitotic checkpoint protein MAD1. Cell. 1998; 93:81–91. [PubMed: 9546394]

Khan SH, Wahl GM. p53 and pRb prevent rereplication in response to microtubule inhibitors by mediating a reversible G1 arrest. Cancer Res. 1998; 58:396–401. [PubMed: 9458079]

Kim S, Park SY, Yong H, Famulski JK, Chae S, Lee JH, Kang CM, Saya H, Chan GK, Cho H. HBV X protein targets hBubR1, which induces dysregulation of the mitotic checkpoint. Oncogene. 2008; 27:3457–3464. [PubMed: 18193091]

Klingelhutz AJ, Roman A. Cellular transformation by human papillomaviruses: Lessons learned by comparing high- and low-risk viruses. Virology. 2012

Levesque AA, Howard L, Gordon MB, Compton DA. A functional relationship between NuMA and kid is involved in both spindle organization and chromosome alignment in vertebrate cells. Mol Biol Cell. 2003; 14:3541–3552. [PubMed: 12972545]

Li R, Murray AW. Feedback control of mitosis in budding yeast. Cell. 1991; 66:519–531. [PubMed: 1651172]

McLaughlin-Drubin ME, Huh KW, Munger K. Human papillomavirus type 16 E7 oncoprotein associates with E2F6. J Virol. 2008; 82:8695–8705. [PubMed: 18579589]

McLaughlin-Drubin ME, Munger K. Oncogenic activities of human papillomaviruses. Virus Res. 2009; 143:195–208. [PubMed: 19540281]

Meraldi P, Draviam VM, Sorger PK. Timing and checkpoints in the regulation of mitotic progression. Dev Cell. 2004; 7:45–60. [PubMed: 15239953]

Musacchio A, Salmon ED. The spindle-assembly checkpoint in space and time. Nat Rev Mol Cell Biol. 2007; 8:379–393. [PubMed: 17426725]

Nguyen CL, McLaughlin-Drubin ME, Munger K. Delocalization of the microtubule motor Dynein from mitotic spindles by the human papillomavirus E7 oncoprotein is not sufficient for induction of multipolar mitoses. Cancer Res. 2008; 68:8715–8722. [PubMed: 18974113]

Nguyen CL, Munger K. Human papillomavirus E7 protein deregulates mitosis via an association with nuclear mitotic apparatus protein 1. J Virol. 2009; 83:1700–1707. [PubMed: 19052088]

Patel D, Incassati A, Wang N, McCance DJ. Human papillomavirus type 16 E6 and E7 cause polyploidy in human keratinocytes and up-regulation of G2-M-phase proteins. Cancer Res. 2004; 64:1299–1306. [PubMed: 14973072]

Peters JM. The anaphase promoting complex/cyclosome: a machine designed to destroy. Nat Rev Mol Cell Biol. 2006; 7:644–656. [PubMed: 16896351]

Piboonniyom SO, Duensing S, Swilling NW, Hasskarl J, Hinds PW, Munger K. Abrogation of the retinoblastoma tumor suppressor checkpoint during keratinocyte immortalization is not sufficient for induction of centrosome-mediated genomic instability. Cancer Res. 2003; 63:476–483. [PubMed: 12543805]

Psyrri A, DeFilippis RA, Edwards AP, Yates KE, Manuelidis L, DiMaio D. Role of the retinoblastoma pathway in senescence triggered by repression of the human papillomavirus E7 protein in cervical carcinoma cells. Cancer Res. 2004; 64:3079–3086. [PubMed: 15126344]

Slebos RJ, Lee MH, Plunkett BS, Kessis TD, Williams BO, Jacks T, Hedrick L, Kastan MB, Cho KR. p53-dependent G1 arrest involves pRB-related proteins and is disrupted by the human papillomavirus 16 E7 oncoprotein. Proc Natl Acad Sci U S A. 1994; 91:5320–5324. [PubMed: 8202487]

Suijkerbuijk SJ, Kops GJ. Preventing aneuploidy: the contribution of mitotic checkpoint proteins. Biochim Biophys Acta. 2008; 1786:24–31. [PubMed: 18472014]

Taylor SS, McKeon F. Kinetochore localization of murine Bub1 is required for normal mitotic timing and checkpoint response to spindle damage. Cell. 1997; 89:727–735. [PubMed: 9182760]

Thomas JT, Laimins LA. Human papillomavirus oncoproteins E6 and E7 independently abrogate the mitotic spindle checkpoint. J Virol. 1998; 72:1131–1137. [PubMed: 9445009]

Wang F, Dai J, Daum JR, Niedzialkowska E, Banerjee B, Stukenberg PT, Gorbsky GJ, Higgins JM. Histone H3 Thr-3 phosphorylation by Haspin positions Aurora B at centromeres in mitosis. Science. 2010; 330:231–235. [PubMed: 20705812]

Zerfass-Thome K, Zwerschke W, Mannhardt B, Tindle R, Botz JW, Jansen-Durr P. Inactivation of the cdk inhibitor p27KIP1 by the human papillomavirus type 16 E7 oncoprotein. Oncogene. 1996; 13:2323–2330. [PubMed: 8957073]

HIGHLIGHTS

- We examined the effect of HPV16 E7 on mitotic checkpoint activity
- E7 inhibited cyclin B degradation
- Multiple E7 domains contribute to this activity
- Inhibition of cyclin B degradation reflects spindle assembly checkpoint engagement
- Spindle assembly checkpoint activation in response to microtubule poisons is normal

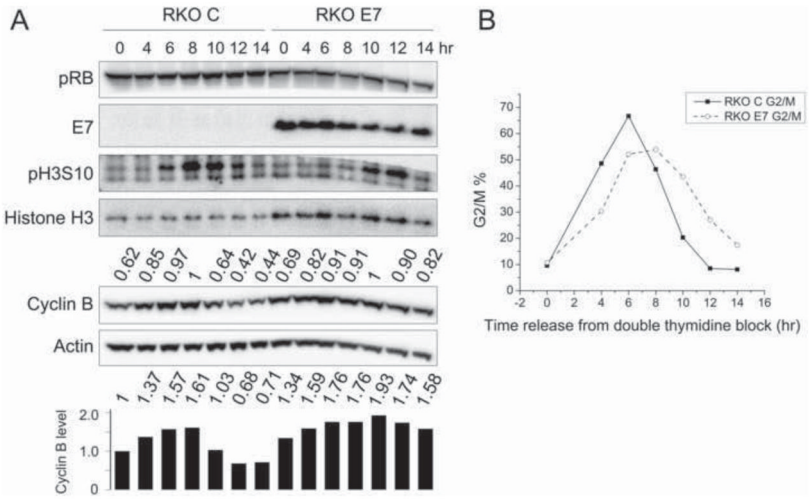

Figure 1. HPV16 E7 expression impedes cyclin B degradation during mitosis in RKO cells

RKO cells with stable expression of empty vector (RKO C) or HPV16 E7 (RKO E7) were collected at different times after release from a double thymidine block. Shown here is a representative experiment; similar results were obtained in two additional experiments. (A) Western blot analyses of pRB, E7, histone H3 phosphorylated at serine 10 (pH3S10), histone H3, cyclin B and actin are shown. Cyclin B quantifications relative to actin are indicated above the cyclin B blot. Values are presented relative to the highest (1) in either RKO C or RKO E7. The bar graph below the actin blot shows the relative cyclin B levels normalized to actin, providing a basis for comparison of RKO C and RKO E7. (B) FACS analyses of G2/M cell populations are shown for RKO C and RKO E7 at different times after release from a double thymidine block.

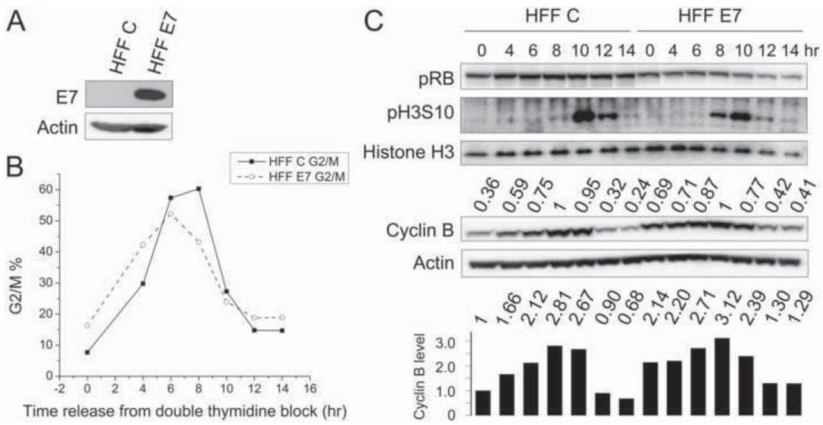

Figure 2. HPV16 E7 expression impedes cyclin B degradation during mitosis in primary human foreskin fibroblasts (HFFs)

HFFs with stable expression of empty vector (HFF C) or HPV16 E7 (HFF E7) were collected at different times after release from a double thymidine block. Shown here is a representative experiment; similar results were obtained in two additional experiments. (A) Western blot analysis of E7 expression in the stable HFF populations. (B) FACS analyses of G2/M cell populations are shown for HFF C and HFF E7 at different times after release from a double thymidine block. (C) Western blot analyses of pRB, pH3S10, histone H3, cyclin B and actin are shown. Cyclin B quantifications relative to actin are indicated above the cyclin B blot. Values are presented relative to the highest (1) in either HFF C or HFF E7. The bar graph below the actin blot shows the relative cyclin B levels normalized to actin, providing a basis for comparison of HFF C and HFF E7.

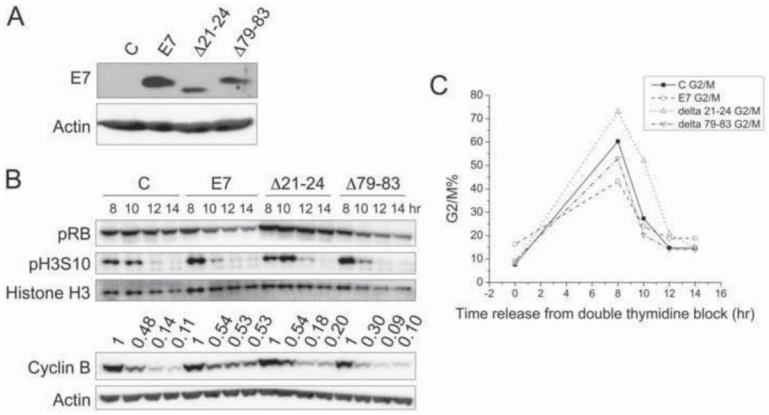

Figure 3. The HPV16 E7Δ21-24 or HPV16 E7Δ79-83 mutants are defective for inhibition of cyclin B degradation during mitosis

HFFs with stable expression of empty vector (C), HPV16 E7 (E7), HPV16 E7Δ21-24 (Δ21-24), or HPV16 E7Δ79-83 (Δ79-83) were collected at different times after release from a double thymidine block. Shown here is a representative experiment; similar results were obtained in three additional experiments with different HFF populations. (A) Western blot analysis of E7 expression in the stable HFF populations. (B) Western blot analyses of pRB, pH3S10, histone H3, cyclin B and actin are shown. Cyclin B quantifications relative to actin are indicated above the cyclin B blot. Values are presented relative to the highest (1) in C, HPV16 E7, HPV16 E7Δ21-24, or HPV16 E7Δ79-83 expressing cells. (C) FACS analyses of G2/M cell populations are shown for HFF C, HPV16 E7, HPV16 E7Δ21-24, and HPV16 E7Δ79-83 expressing cells at different times after release from a double thymidine block.

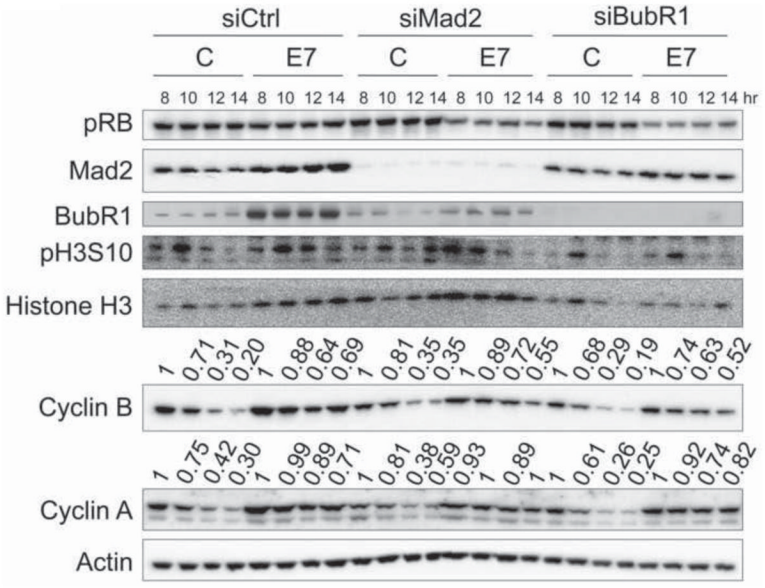

Figure 4. HPV16 E7 impedes the degradation of mitotic cyclins through SAC-dependent and SAC-independent mechanisms

HFFs with stable expression of empty vector (C) or HPV16 E7 (E7) were transfected with non-targeting control siRNAs, siMad2, or siBubR1 before subjected to a double thymidine block. Western blot analyses of pRB, Mad2, BubR1, pH3S10, histone H3, cyclin B, cyclin A and actin are shown. Cyclin B and cyclin A quantifications relative to actin are indicated above the respective blots. Values are presented relative to the highest (1) in each condition. Shown here is a representative experiment; similar results were obtained in three additional experiments.

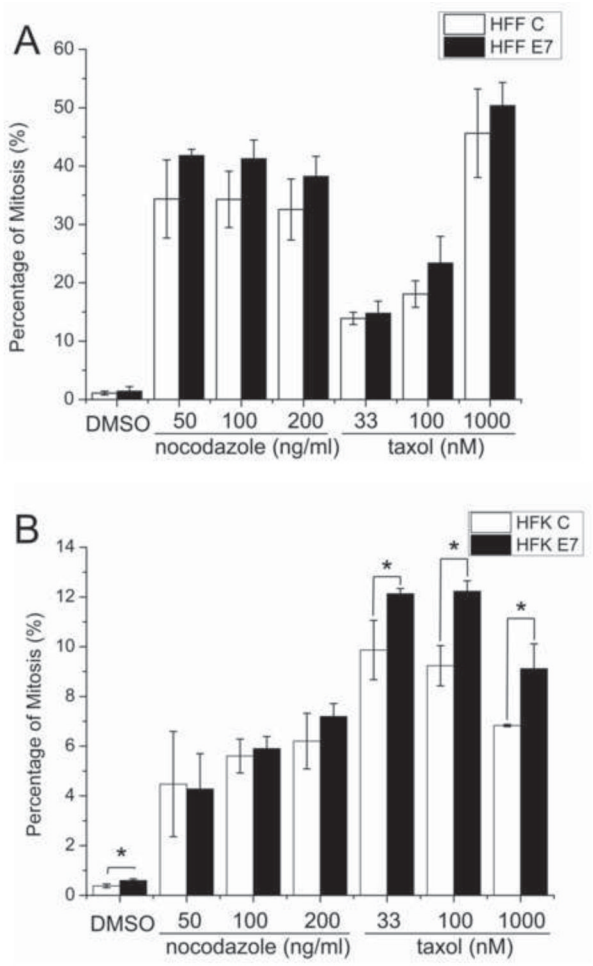

Figure 5. HPV16 E7 expression does not compromise the SAC response to microtubule poisons

(A) HFFs with stable expression of empty vector (HFF C) or HPV16 E7 (HFF E7) were G1/S arrested by treating with thymidine for 24 hours and released into medium containing DMSO, nocodazole, or taxol at the indicated concentrations for 18 hours. (B) HFKs with stable expression of empty vector (HFK C) or HPV16 E7 were treated with DMSO, nocodazole, or taxol at the indicated concentrations for 24 hours. Mitotic indices were determined by FACS analyses with MPM-2 and propidium iodide staining. The bar graph shows averages and standard deviations from three independent experiments. Statistically significant differences ($P < 0.05$) between control and E7 expressing HFKs as determined by Student's t-test are denoted by an asterisk.